Abdominal Radiology (2019) 44:1873–1882
https://doi.org/10.1007/s00261-018-1882-8

PELVIS

Prenatal planning of placenta previa: diagnostic accuracy of a novel MRI-based prediction model for placenta accreta spectrum (PAS) and clinical outcome

Andrea Delli Pizzi[1] · Alessandra Tavoletta[2] · Roberta Narciso[2] · Domenico Mastrodicasa[3] · Stefano Trebeschi[4] · Claudio Celentano[5] · Jacopo Mastracchio[6] · Roberta Cianci[2] · Barbara Seccia[2] · Luisa Marrone[6] · Marco Liberati[6] · Antonio Raffaele Cotroneo[1,2] · Massimo Caulo[1,2] · Raffaella Basilico[2]

Published online: 1 January 2019
© Springer Science+Business Media, LLC, part of Springer Nature 2019

Abstract

Purpose To investigate the diagnostic accuracy of MRI for placenta accreta spectrum (PAS) and clinical outcome prediction in women with placenta previa, using a novel MRI-based predictive model.

Methods Thirty-eight placental MRI exams performed on a 1.5T scanner were retrospectively reviewed by two radiologists in consensus. The presence of T2 dark bands, myometrial thinning, abnormal vascularity, uterine bulging, placental heterogeneity, placental protrusion sign, placental recess, and percretism signs was scored using a 5-point scale. Pathology and clinical intrapartum findings were the standard of reference for PAS, while intrapartum/peripartum bleeding and emergency hysterectomy defined the clinical outcome. Receiver-operating characteristic (ROC) analysis and discriminant function analysis were performed to test the predictive power of MRI findings for both PAS and clinical outcome prediction.

Results Abnormal vascularity and percretism signs were the two most predictive MRI features of PAS. The area under the curve (AUC) of the predictive function was 0.833 (cutoff 0.39, 67% sensitivity, 100% specificity, $p = 0.001$). Percretism signs and myometrial thinning were the two most predictive MRI features of poor outcome. AUC of the predictive function was 0.971 (cutoff −0.55, 100% sensitivity, 77% specificity, $p < 0.001$).

Conclusion The diagnostic accuracy of MRI, especially considering the combination of the most predictive MRI findings, is higher when the target of the prediction is the clinical outcome rather than the PAS.

Keywords Magnetic resonance · Placenta accreta spectrum (PAS) · Placenta previa · Placental invasion · Intrapartum bleeding · Clinical outcome

✉ Andrea Delli Pizzi
andreadellipizzi@gmail.com

[1] ITAB Institute of Advanced Biomedical Technologies, "G. d'Annunzio" University, Via Luigi Polacchi 11, 66100 Chieti, Italy

[2] Department of Neuroscience, Imaging and Clinical Sciences, "G. d'Annunzio" University, Chieti, Italy

[3] Department of Radiology, Stanford University School of Medicine, 300 Pasteur Dr, S-072, Stanford, CA 94305-5105, USA

[4] Department of Radiology, Netherlands Cancer Institute, Amsterdam, The Netherlands

[5] Department of Medicine and Ageing Sciences, G. d'Annunzio University of Chieti-Pescara, Chieti, Italy

[6] Department of Obstetrics and Gynaecology, G. d'Annunzio University of Chieti-Pescara, Chieti, Italy

Introduction

Placenta accreta spectrum (PAS) is the general term applied to abnormal adherence of the placental trophoblast to the uterine placenta. The spectrum includes the attachment of the placenta to myometrium without intervening decidua (placenta accreta), the invasion of the myometrium (placenta increta), and the infiltration of the surrounding organs through the uterine serosa (placenta percreta) [1]. Previous cesarean section and placenta previa are the two most important risk factors [2]. Pregnancies with invasive placenta are more likely to have a preterm delivery and develop potentially fatal (7% cases) massive bleeding caused by the abnormal invasion of the uterus by the placenta [3, 4]. More in detail, placental implantation abnormalities, including placenta previa and placenta accreta, can have catastrophic

consequences for both mother and fetus, especially as pregnancy progresses to term [5]. The damage of myometrial circulation by the placental invasion is responsible for maternal bleeding and potential fetal compromise [6]. The presence of placenta previa represents a risk factor for vasa previa and premature rupture of membranes (PROM) that can lead to vessel tearing and rapid fetal bleeding [5]. Moreover, placenta previa is associated with dysregulated interface function (cell-free human placental lactogen mRNA is elevated in maternal circulation of these patients) leading to an increased risk of fetomaternal hemorrhage [7].

Up to 40–60% of the peripartum hysterectomies are due to invasive placenta [8]. The International Federation of Gynecology and Obstetrics (FIGO) recently developed guidelines and recommendations to improve the diagnosis and the management (conservative versus nonconservative) of PAS disorders, thus reducing the burden of maternal mortality and long-*term sequelae that arise from this disease* [9–13].

In this context, the prenatal diagnosis of invasive placenta plays an essential role in the delivery management. Although ultrasound (US) still represents the first-line examination for the antenatal care, a growing interest toward magnetic resonance (MR) imaging was developed in recent years [14, 15]. In fact, compared with US, MR has the advantage of high soft tissue contrast resolution and provides a panoramic view of the tissues and organs surrounding the uterus. In this way, it can be helpful to add topographic and morphologic information representing a complementary tool in cases with equivocal ultrasound findings or when additional information is needed [14, 16, 17]. Moreover, several studies described some MR-predictive "signs" of placental invasion, such as the presence of dark intraplacental bands in T2-weighted (T2w) images, myometrial thinning, heterogeneous placental signal intensity, placental protrusion sign, abnormal uterine bulging sign, abnormal placental vascularity, placental recess, tenting of the bladder, and/or infiltration of pelvic organs (Table 1) [18–27]. In this regard, a recently published study investigated the potential role of the MR to predict the clinical outcome in terms of treatment (conservative or not) and bleeding (massive or minor) of women with invasive placenta previa [26]. However, none of the above mentioned studies investigated the best combination of predictive MR signs correlating MR findings with both PAS and clinical outcome.

Therefore, the aim of our study was to investigate the diagnostic accuracy of MRI for PAS diagnosis and clinical outcome prediction in women with placenta previa, using a novel MRI-based predictive model.

Methods

Patients

All our procedures involving human subjects were in accordance with the ethical standards of the institutional and/or national research committee and with the 1964 Helsinki declaration and its later amendments or comparable ethical standards. All imaging data were retrospectively retrieved from PACS and informed consent was waived.

Fifty consecutive parturients with placenta previa and clinically and/or ultrasound suspect of PAS from June 2014 to May 2017 were retrospectively selected.

Inclusion criteria were (1) availability of MR imaging and (2) surgery outcome/pathology.

Among *the fifty potentially eligible patients*, 12 were excluded. More specifically, nine were excluded due to patient transfer to another facility/hospital before deliver, *one had vaginal delivery*, one had to undergo emergency delivery before MR examination and in one case, the ultrasound findings of placenta previa were not confirmed by the MR exam.

Finally, a total of 38 patients (median age 36 years; range 21–44) were included in the study. *All the MR exams were performed within a week from the US examination.* The

Table 1 MR-predictive "signs" of PAS

MR signs	
Intraplacental T2 dark bands	Band-shaped low signal intensity lines in the placenta
Myometrial thinning	Focal defect of the hypointense uteroplacental interface with myometrial thinning
Heterogeneous placental signal intensity	Heterogeneous intensity within the placenta due to hemorrhage or vascular lacunae
Placental Protrusion sign	Placental extension and projection into the internal uterine os
Uterine bulging	Uterine enlargement of the fundus and wider appearance of the body than the caudal segments
Abnormal placental vascularity	Enlarged and tortuous vessels represented by flow void signals within the placenta on T2w images
Placental recess	Wedge-shaped contraction of the placental surface and uterine outer rim accompanying a T2 dark band
Percretism signs	"Tenting" of the bladder and/or infiltration of pelvic organs

baseline characteristics of all patients included in this study are shown in Fig. 1.

MRI technique

The MRI studies were performed on a 1.5T Scanner (Achieva, Philips Medical System, Best, the Netherlands). MR protocol comprised T2w images (including high resolution sequences) in sagittal, coronal, and axial orientations using a fast spin-echo sequence; T1-Thrive sequences were obtained in axial plane. MR protocols and sequence parameters are summarized in Table 2.

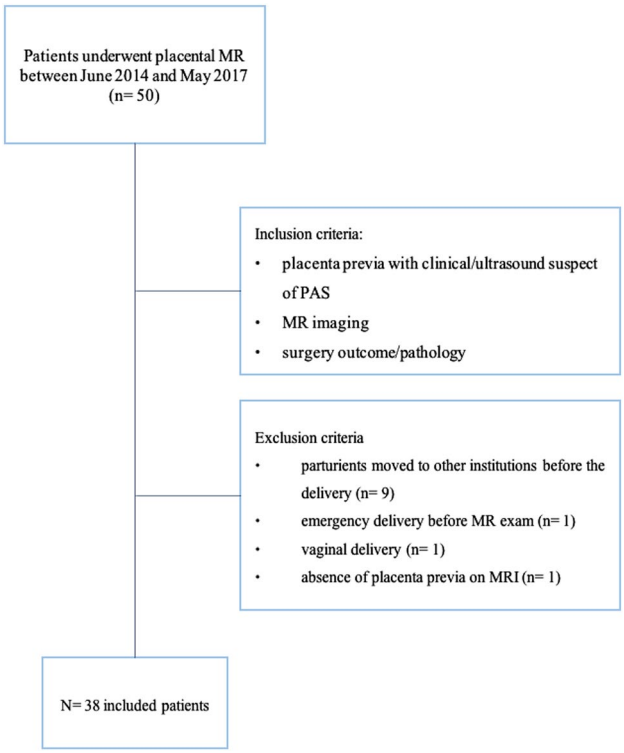

Fig. 1 Flowchart of the study population

Imaging analysis

Two radiologists, with at least 5 years of experience in abdominal imaging MR, in consensus, reviewed the MR images assessing the following features (Fig. 2):

1. Intraplacental T2 dark bands: band-shaped low signal intensity lines in the placenta ≥ 2 cm (Fig. 2a) [18].
2. Myometrial thinning: focal defect of the hypointense uteroplacental interface with myometrial thinning or indistinctness of myometrial delineation on T2w images (Fig. 2b) [18, 22].
3. Intraplacental abnormal vascularization: enlarged and tortuous vessels represented by flow void signals with a diameter > 6 mm within the placenta on T2w images (Fig. 2c) [20].
4. Uterine bulging: loss of normal "pear shape" of the uterus, with the enlargement of the fundus and the wider appearance of the body than the caudal segments (Fig. 2d) [18, 19].
5. Heterogenous intraplacental sign: heterogeneous intensity within the placenta due to hemorrhage or vascular lacunae (Fig. 2e) [18, 23].
6. Placental protrusion sign: the placenta extend and project into the internal uterine os (Fig. 2f) [21].
7. Placental recess: it is described as a placental deformity with the contraction of the placental surface and uterine outer rim. It shows a wedge-shaped contour and accompanies a T2 dark band (Fig. 2g) [24].
8. Percretism signs: direct invasion of adjacent organs (bladder or rectum) (Fig. 2h) [19].

Table 2 MR sequences and parameters used for the study

	T2-weighted Ssh[a] Sagittal	T2-weighted Ssh[a] Coronal	T2-weighted Ssh[a] Axial	T2-weighted TSE HR[b] Sagittal	T1-thrive Axial
TR/TE (ms)	648/80	648/80	656/80	3823/90	3.9/1.85
Slice thickness (mm)	5	5	5	4	4
Flip angle	90	90	90	90	10
Reconstruction matrix	256	256	384	384	256
Scan mode	2D	2D	2D	2D	3D
Fat suppression	No	No	No	No	Yes
Field of view (mm)	315×276	315×276	385×349	280×280	375×293
Acquisition time (min)	00.29″	00.22″	00.26″	02.25″	01.10″
No. of sections	45	34	40	35	120

[a]Single shot

[b]Turbo spin echo high resolution

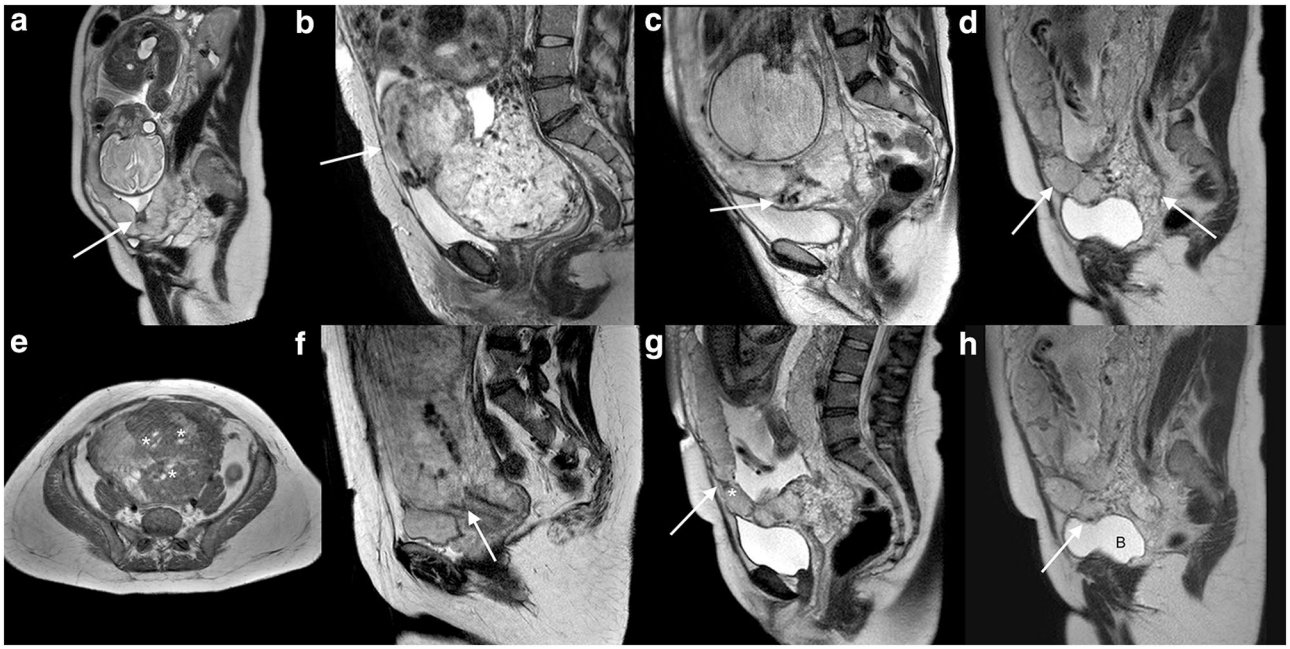

Fig. 2 Sagittal T2-weighted (**a**–**d**, **f**–**h**) and axial T1-weighted (**e**) images showing MRI criteria. **a** Intraplacental dark band (white arrow) with the major diameter longer than 2 cm. **b** Myometrial thinning (white arrow): focal defect of the hypointense uteroplacental interface with myometrial thinning or indistinctness of myometrial delineation. **c** Intraplacental abnormal vascularity: enlarged and tortuous vessels (white arrow) with a diameter > 6 mm. **d** Uterine bulging (white arrows): loss of normal "pear shape" of the uterus, with the wider appearance of the body than the caudal segments. **e** Heterogenous intraplacental sign: heterogeneous intensity within the placenta due to hemorrhage or vascular lacunae (white asterisks). **f** Placental protrusion sign: the placenta extends and projects (white arrow) into the internal uterine os. **g** Placental recess: the contraction of the placental (white arrow) surface accompanying a dark band (white asterisk). **h** Percretism signs: direct invasion (white arrow) of bladder (**b**)

The presence of each MR sign was qualitatively assessed according to a 5-point scale: 1 = absent, 2 = probably absent, 3 = indeterminate, 4 = probably present, and 5 = certainly present.

In case of disagreement, the two readers reviewed MR images for a second time after 2 weeks. If the disagreement persisted, a third radiologist (with 15 years of experience in abdominal imaging MR) decided the final score.

Standard of reference

Both "pathology reports" and "clinical intrapartum findings" were used as standard of reference to confirm the presence of invasive placenta. The clinical outcome was assessed after a multidisciplinary team (gynecologists and radiologists) consensus based on clinically records. The poor-outcome group was defined as parturient with massive intrapartum/peripartum bleeding (> 1000 ml) and/or emergency hysterectomy (nonconservative management). The good outcome group was defined as parturient with minor intrapartum/peripartum hemorrhage (≤ 1000 ml) and preserved uterus (conservative management).

Statistical analysis

The frequency distribution of qualitative MRI features regarding the presence/absence of invasive placenta and poor/good clinical outcome was calculated by using Fisher exact test. Qualitative scores were dichotomized considering 1, 2, 3 as negative scores and 4, 5 as positive rating. The diagnostic power of each MR feature was calculated by receiver-operating characteristic (ROC) curve analysis. All the MR features were included in a stepwise discriminant function analysis. This analysis was conducted to determine whether a set of variables is effective in predicting category membership. Wilks' lambda was the variable selection method and F value was the criterion for entry and removal from the equation. In this way, at each step the variable that minimizes the overall Wilks' lambda is included in the model. Coefficients were also determined indicating the unique contribution of each variable to the predictive function. Finally, a ROC curve analysis of the predictive function (both for invasive placenta and for clinical outcome) was used to determine a cutoff with relative sensitivity and specificity. A p value ≤ 0.05 was considered statistically significant. All statistical analyses

were performed by using IBM SPSS Statistics software, version 20 (IBM, Armonk, NY).

Results

Out of 38 patients, 12 (31.6%) were diagnosed with PAS (6 with *placenta accreta* and 6 with *placenta percreta*) and 26 (68.4%) did not show PAS. When considering the clinical outcome, 8 (21.1%) parturient underwent emergency hysterectomy and/or blood transfusion due to massive bleeding (> 1000 ml) and 30 (78.9%) showed minor intrapartum/peripartum hemorrhage (≤ 1000 ml) and preserved uterus (Figs. 3, 4). In detail, all the 6 patients that revealed PAS with *placenta percreta* at pathology underwent emergency isterectomy. Further patient characteristics are summarized in Table 3.

The readers showed disagreement in five patients. In three of them, it concerned the myometrial thinning, and in two, it regarded the uterine bulging sign. In all the five cases, the third radiologist decided the final score.

The results of frequency distribution and the diagnostic accuracy (by means AUC and ROC curve) of each MR sign regarding PAS and clinical outcome are shown in Table 4. None of the 38 parturients showed the placental protrusion sign at MRI examinations. This MR sign was excluded from the further analysis.

Diagnostic performances of the predictive models are summarized in Table 5 and Fig. 5. The Discriminant Analysis provided two specific predictive models, one for the PAS diagnosis (present in 12/38 patients) and the other for the clinical outcome (delivery management) prediction (8/38 patients with nonconservative management). In detail, the predictive model selected two MR signs for the predictive function of PAS: intraplacental abnormal vascularity and percretism signs. AUC of the predictive model for PAS was 0.833 with a cutoff of 0.39 (67% sensitivity and 100% specificity, $p = 0.001$). When considering the predictive function of clinical outcome, myometrial thinning and percretism signs were selected. AUC of the predictive model for clinical outcome was 0.971 with a cutoff of −0.55 (100% sensitivity and 77% specificity, $p < 0.001$).

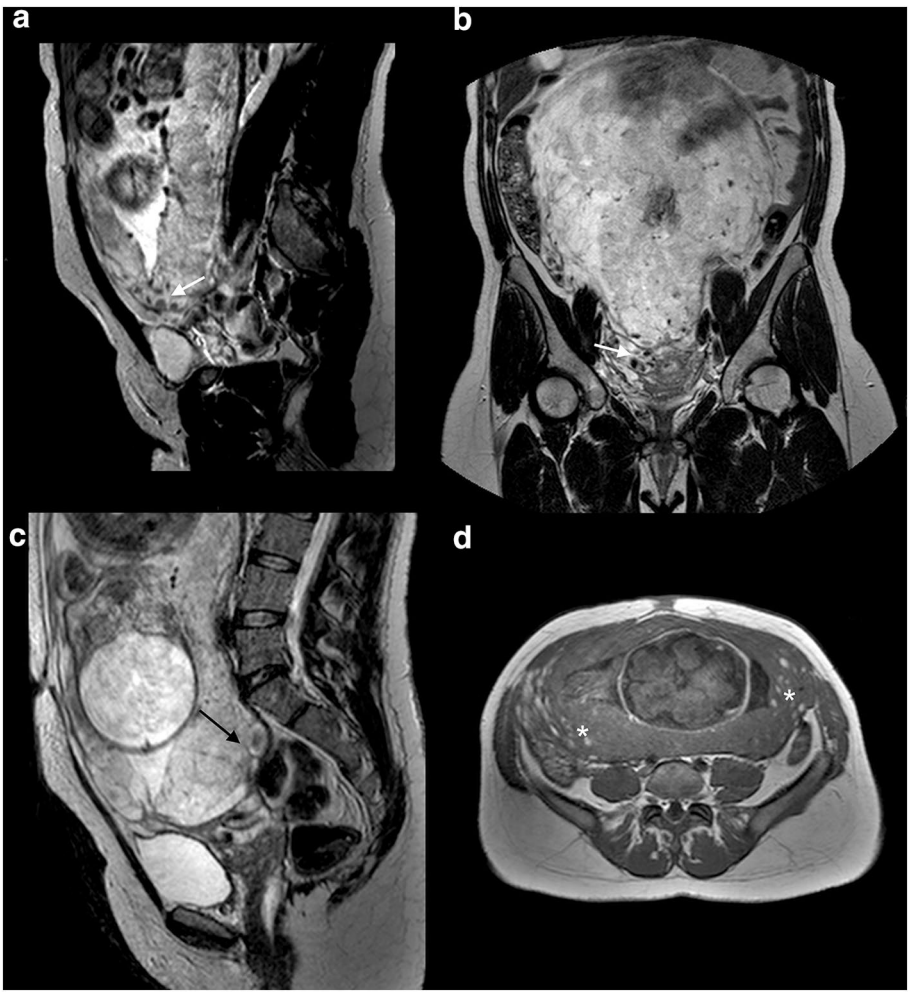

Fig. 3 A case of good outcome in a 33-year-old pregnant with invasive placenta. Sagittal (**a**, **c**) and coronal (**b**) T2-weighted images and axial T1-weighted image (**d**) showing abnormal flow voids (white arrow in **a** and **b**), uterine bulging (black arrow in **c**) and heterogeneous signal intensity due to focal hemorrhage (white asterisks in **d**). The patient had minor bleeding and underwent conservative treatment (bakri balloon and b-lynch suture). Invasive placenta with accretism was demonstrated at the delivery

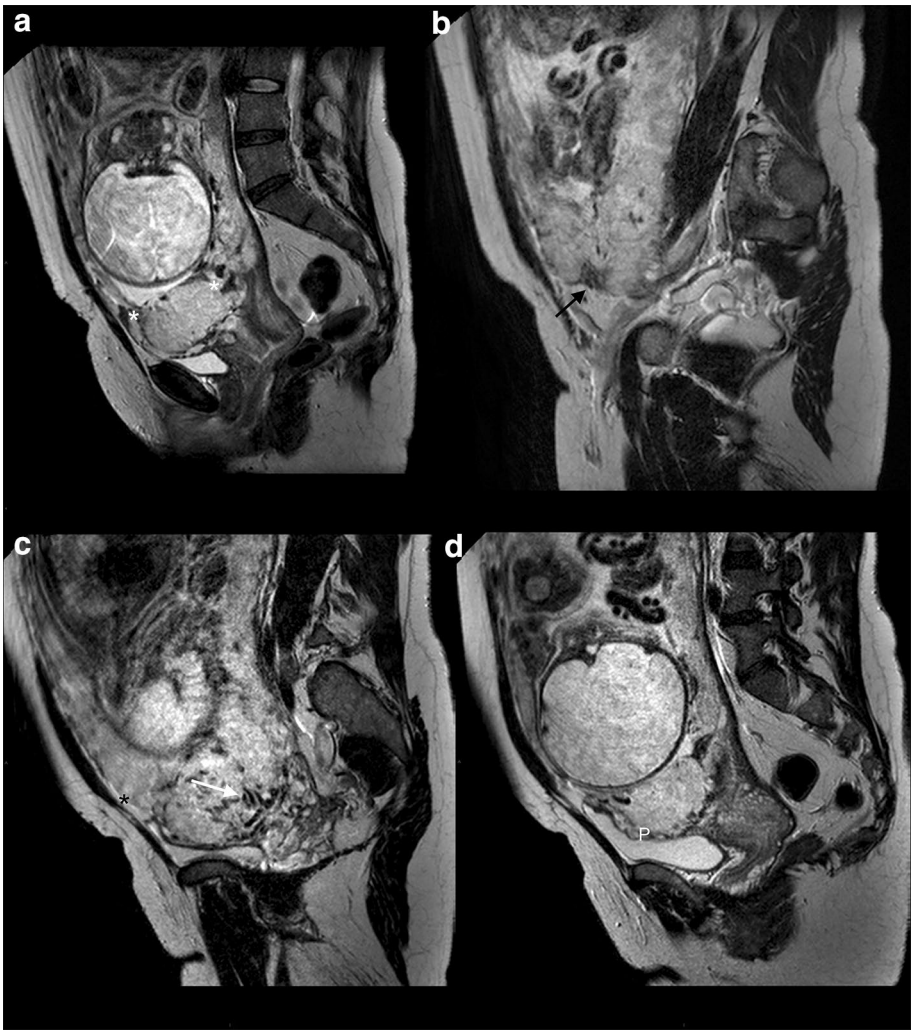

Fig. 4 A case of poor outcome in a 36-year-old pregnant with invasive placenta. Sagittal (**a**–**d**) T2-weighted images showing intraplacental dark bands (white asterisks in **a**), placental recess (black arrow in **b**), intraplacental abnormal vascularity (white arrow in **c**), myometrial thinning with focal indistinctness of its delineation (black asterisk in **c**) and signs of percretism with bladder invasion (white P″ in **d**). The patient underwent emergency hysterectomy and PAS with percretism was histologically confirmed

Discussion

The aim of our study was to investigate the role of MR for the PAS diagnosis and the clinical outcome prediction in the prenatal planning of women with placenta previa. Our results demonstrated that the diagnostic performance of MR improves when the MR findings are combined to predict the conservative versus nonconservative management. The rationale of this approach was that the delivery management prediction may represent an added value in the delivery management. In fact, treatment strategies for PAS depend not only on the presence or absence of invasive placenta but mostly on the type of PAS (presence or not of adjacent organ invasion) and on the entity of bleeding. For instance, they range from conservative strategies (urotonics, intrauterine balloon tamponade, and uterine artery embolization) to the hysterectomy in case of parturients with adjacent organ invasion or massive bleeding [28]. In addition, if, on the one hand, the presence of invasive placenta represents a risk factor for massive bleeding, on the other hand, not all intrapartum/peripartum bleeding are uniquely related to the presence of invasive placenta. In this regard, the delivery management may be influenced also by other causes of uterine hemorrhage including lack of uterine tone (not predictable with MR), lacerations, retained placental tissue, uterine inversion, infection, and coagulation defects [29].

In this context, in this study, the diagnostic performance improved considering the MR findings taken individually and combining the MR findings with the best diagnostic performances in a developed predictive model. In detail, percretism signs were found to be the most important predictive variable, both considering the PAS and the clinical outcome prediction. When the percretism signs were combined with myometrial thinning they differentiated parturients that underwent hysterectomy and/or intrapartum/peripartum massive bleeding with an AUC of 0.971 ($p < 0.001$). On the other hand, when percretism signs were combined with intraplacental abnormal vascularity, they predicted the presence of PAS with an AUC of 0.833 ($p = 0.001$). Interestingly, the predictive power increased in terms of sensitivity

Table 3 Baseline demographic and clinical characteristics of participants

Variable	Value
Median age (range)	36 (21–44)
Median weeks of gestation (SD)	33 (2)
Risk factors for PAS	
None	25
CS	15
UCR	17
Smoke/drugs	5
Median gestational age (range)	33 (29-38)
Clinical outcome[a]	
Good	30
Poor	8
PAS[b]	
Absent	26
Present	12

CS cesarean section, *UCR* uterine cavity revision, *PAS* placenta accreta spectrum

[a]Good Clinical Outcome = minor intrapartum/peripartum hemorrhage (≤1000 ml) and preserved uterus; Poor Clinical Outcome = massive intrapartum/peripartum bleeding (> 1000 ml) and/or emergency hysterectomy

[b]PAS was assessed on "pathology reports" and/or "clinical intrapartum findings"

Table 4 Diagnostic accuracies of MR findings for "PAS" and "clinical outcome"

MR findings	*p*-value*	ROC curve analysis	
		AUC (SE**)	*p*-value
Intraplacental T2 dark bands			
PAS	0.157	0.638 (0.099)	0.177
Clinical outcome	0.003	0.804 (0.085)	0.009
Myometrial thinning			
PAS	0.481	0.577 (0.102)	0.451
Clinical outcome	< 0.001	0.883 (0.053)	0.001
Intraplacental abnormal vascularization			
PAS	< 0.001	0.750 (0.098)	0.014
Clinical outcome	< 0.001	0.717 (0.118)	0.063
Uterine bulging			
PAS	0.045	0.673 (0.100)	0.090
Clinical outcome	0.002	0.808 (0.097)	0.008
Heterogeneous intraplacental sign			
PAS	0.164	0.641 (0.097)	0.167
Clinical outcome	0.117	0.675 (0.105)	0.133
Placental recess			
PAS	0.002	0.731 (0.099)	0.024
Clinical outcome	< 0.001	0.858 (0.095)	0.002
Percretism signs			
PAS	< 0.001	0.750 (0.098)	0.014
Clinical outcome	< 0.001	0.875 (0.094)	0.001

ROC receiver-operating characteristic curve, *AUC* area under the ROC curve

*Fisher's exact test

**Standard error

(from 67 to 100%) if the subject moves from the PAS to the clinical outcome, meaning that none of poor-outcome patients was missed. These results may have a beneficial effect from a clinical point of view because they focus the attention on "critical" patients, thus representing an alarm for clinicians, allowing to arrange in advance blood products and the most appropriate surgical team. In this context, the solely placental invasion prediction may result "incomplete" since not all the PAS develop massive bleeding and needs of hysterectomy. In fact, in our study population, 33% (4/12) of PAS was treated conservatively *using uterotonics, intrauterine balloon tamponade, and/or uterine artery embolization.*

Looking at MR findings individually, intraplacental dark band, myometrial thinning, intraplacental abnormal vascularity, uterine bulging, placental recess, and percretism signs showed significant differences between women having poor clinical outcome and good clinical outcome. More in detail, myometrial thinning, percretism signs, and placental recess showed the highest diagnostic accuracy (AUC of 0.883, 0.875, and 0.858, respectively). To the best of our knowledge, the study by Chen et al., recently published, was the only one investigating the potential role of MRI findings for the prediction of clinical outcome [26]. The chosen criteria to define good and poor clinical outcomes (massive/minor bleeding and conservative treatment/hysterectomy) were the same as in the study. They demonstrated that dark band, percretism signs, and placental protrusion signs were more frequently observed in patients with poor outcome and that dark band was the only significant predictor of poor outcome. Compared to their results, in our study percretism signs showed a 4-times greater predictive power (Table 5) compared to the second variable selected (myometrial thinning). We hypothesize that two factors may explain the differences with Chen et al's study. First of all, the study population is different. In fact, Chen et al. included only women who underwent uterine artery embolization-assisted cesarean section. Second, some differences in the criteria for the image analysis existed. For example, they did not evaluate the placental recess and intraplacental abnormal vascularity. Furthermore, the definitions of MRI findings were slightly different compared to ours. For instance, we considered dark band as present only when they were equal or greater than 2 cm in accordance with that of Lax et al., while they (Chen et al) assessed the presence of dark band regardless of any dimensional limit [18].

Table 5 Stepwise discriminant analysis and ROC curve analysis of the predictive functions

	MR Findings	Stepwise discriminant analysis				ROC curve analysis of the predictive function				
		Unstandardized coefficients	Constant	Wilks' lambda	*p*-value	AUC (SE)	*p*-value	Cutoff	Sensitivity (%)	Specificity (%)
PAS	Intraplacental abnormal vascularity	2.121	−0.670	0.494	< 0.001	0.833 (0.086)	0.001	0.39	67	100
	Percretism signs	2.121								
Clinical outcome	Myometrial thinning	1.231	−1.167	0.246	< 0.001	0.971 (0.026)	< 0.001	−0.55	100	77
	Percretism signs	4.310								

SE standard error

When considering the PAS, intraplacental abnormal vascularity and percretism signs showed the best diagnostic accuracy (AUC = 0.750, $p = 0.014$) followed by placental recess (AUC = 0.731, $p = 0.024$). These results are in line with those of Derman et al. that in 2011 first identified the presence of enlarged tortuous flow voids on T2-weighted images as MR criterion of placental invasion [20]. Ueno et al. hypothesized that the intraplacental abnormal vascularity was related to the abnormal development of maternal arteries where the placenta adheres closely to the myometrium with subsequent infiltration of the placenta [21]. Placental recess was a more recently defined MR finding consisting of a wedge-shaped placental deformity accompanied by a dark band. It showed promising results with high accuracy for the diagnosis of placental invasion [24]. The first MRI-based predictive model for the placental invasion was developed by Ueno et al. in 2016, and included abnormal vascularity, dark band, uterine bulging, heterogeneous placenta, placental protrusion sign, and myometrial thinning [27]. Compared to their results, in our study, we did not observe significant differences between the two groups in terms of dark band, myometrial thinning, heterogeneous placenta, and placental protrusion sign. In this regard, no parturients with placental protrusion sign were observed in our study, probably due to the small number of invasive placenta included in our population. In accordance with recent studies demonstrating that the prediction of placental invasions improved when at least two MRI signs are combined together, our stepwise discriminant analysis selected two MRI findings (percretism signs and intraplacental abnormal vascularity) for the predictive function [25, 30]. The specificity of this function is, however, burdened with a relatively lower sensitivity meaning that 34% (4/12) of PAS were missed. This percentage is nonetheless higher than that reported by Sato et al. (22% for abnormal vascularity) and comparable to that described by Valentini et al. (75% for intraplacental abnormal vascularity and of 50% for percretism signs) [24, 25].

We are aware that this study has a few limitations. First of all, due to the fact that PAS and poor clinical outcome *(nonconservative management)* represent relatively rare conditions, our sample size is relatively small, and this may have affected the results of statistical analysis. In this regard, we adopted restrictive selection criteria by including only patients with placenta previa to increase the homogeneity of our study population. Second, the MRI findings used in our study were established according to the recent literature. However, as discussed above, a certain grade of heterogeneity is undoubtedly still present and should be considered when comparing our results to those of other studies. Third, due to the retrospective nature of the study, our results should be considered as preliminary report for future large perspective researches.

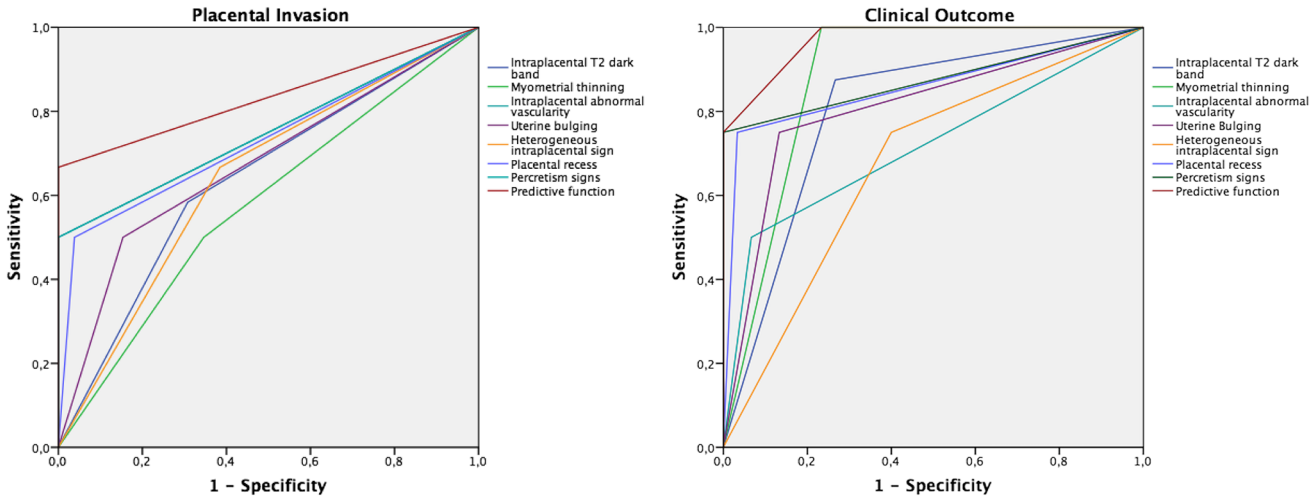

Fig. 5 ROC curve analysis of MR findings and predictive functions for PAS and clinical outcome

Conclusions

In conclusion, the diagnostic performance of MRI is higher when the target is the clinical outcome prediction rather than the PAS diagnosis. In particular, the combination of two MR findings, namely percretism signs and myometrial thinning for clinical outcome, and percretism signs and intraplacental abnormal vascularity for PAS, reached a higher diagnostic accuracy compared to that of the individual findings. Further studies are warranted to confirm these results in larger sample size.

Author contributions All authors were involved in patient management and wrote and/or reviewed the report. Written consent to publication was obtained.

Compliance with ethical standards

Conflict of interest All authors declare that they have no conflict of interest.

Ethical approval All procedures performed in this study involving human participant were in accordance with the ethical standards of the institutional and/or national research committee and with the 1964 Helsinki declaration and its later amendments or comparable ethical standards.

Informed consent Informed consent was obtained from the patients included in this study.

References

1. Silver, R.M. and D.W. Branch, *Placenta Accreta Spectrum*. N Engl J Med, 2018. **378**(16): p. 1529-1536.
2. Higgins, M.F., et al., *Real increasing incidence of hysterectomy for placenta accreta following previous caesarean section*. Eur J Obstet Gynecol Reprod Biol, 2013. **171**(1): p. 54-6.
3. Committee on Obstetric, P., *Committee opinion no. 529: placenta accreta.* Obstet Gynecol, 2012. **120**(1): p. 207-11.
4. Hudon, L., M.A. Belfort, and D.R. Broome, *Diagnosis and management of placenta percreta: a review*. Obstet Gynecol Surv, 1998. **53**(8): p. 509-17.
5. Vintzileos, A.M., C.V. Ananth, and J.C. Smulian, *Using ultrasound in the clinical management of placental implantation abnormalities*. Am J Obstet Gynecol, 2015. 213(4 Suppl): p. S70-7.
6. Jauniaux, E., S. Collins, and G.J. Burton, Placenta accreta spectrum: pathophysiology and evidence-based anatomy for prenatal ultrasound imaging. *Am J Obstet Gynecol*, 2018. **218**(1): p. 75-87.
7. Umazume, T., et al., *Occult fetomaternal hemorrhage in women with pathological placenta with respect to permeability*. J Obstet Gynaecol Res, 2016. **42**(6): p. 632-9.
8. D'Arpe, S., et al., *Emergency peripartum hysterectomy in a tertiary teaching hospital: a 14-year review*. Arch Gynecol Obstet, 2015. **291**(4): p. 841-7.
9. Allen, L., et al., *FIGO consensus guidelines on placenta accreta spectrum disorders: Nonconservative surgical management*. Int J Gynaecol Obstet, 2018. **140**(3): p. 281-290.
10. Sentilhes, L., et al., *FIGO consensus guidelines on placenta accreta spectrum disorders: Conservative management*. Int J Gynaecol Obstet, 2018. **140**(3): p. 291-298.
11. Jauniaux, E., et al., *FIGO consensus guidelines on placenta accreta spectrum disorders: Introduction*. Int J Gynaecol Obstet, 2018. **140**(3): p. 261-264.
12. Jauniaux, E., et al., *FIGO consensus guidelines on placenta accreta spectrum disorders: Prenatal diagnosis and screening*. Int J Gynaecol Obstet, 2018. **140**(3): p. 274-280.
13. Jauniaux, E., et al., *FIGO consensus guidelines on placenta accreta spectrum disorders: Epidemiology*. Int J Gynaecol Obstet, 2018. **140**(3): p. 265-273.
14. Fadl, S., et al., *Placental Imaging: Normal Appearance with Review of Pathologic Findings*. Radiographics, 2017. **37**(3): p. 979-998.
15. Rahaim, N.S. and E.H. Whitby, *The MRI features of placental adhesion disorder and their diagnostic significance: systematic review*. Clin Radiol, 2015. **70**(9): p. 917-25.

16. Zaidi, S.F., et al., *Comprehensive Imaging Review of Abnormalities of the Placenta*. Ultrasound Q, 2016. **32**(1): p. 25-42.
17. Blaicher, W., et al., *Magnetic resonance imaging of the normal placenta*. Eur J Radiol, 2006. **57**(2): p. 256-60.
18. Lax, A., et al., *The value of specific MRI features in the evaluation of suspected placental invasion*. Magn Reson Imaging, 2007. **25**(1): p. 87-93.
19. Baughman, W.C., J.E. Corteville, and R.R. Shah, *Placenta accreta: spectrum of US and MR imaging findings*. Radiographics, 2008. **28**(7): p. 1905-16.
20. Derman, A.Y., et al., *MRI of placenta accreta: a new imaging perspective*. AJR Am J Roentgenol, 2011. **197**(6): p. 1514-21.
21. Ueno, Y., et al., *Novel MRI finding for diagnosis of invasive placenta praevia: evaluation of findings for 65 patients using clinical and histopathological correlations*. Eur Radiol, 2014. **24**(4): p. 881-8.
22. Bour, L., et al., *Suspected invasive placenta: evaluation with magnetic resonance imaging*. Eur Radiol, 2014. **24**(12): p. 3150-60.
23. Masselli, G. and G. Gualdi, *MR imaging of the placenta: what a radiologist should know*. Abdom Imaging, 2013. **38**(3): p. 573-87.
24. Sato, T., et al., *Placental recess accompanied by a T2 dark band: a new finding for diagnosing placental invasion*. Abdom Radiol (NY), 2017. **42**(8): p. 2146-2153.
25. Valentini, A.L., et al., *The morbidly adherent placenta: when and what association of signs can improve MRI diagnosis? Our experience*. Diagn Interv Radiol, 2017. **23**(3): p. 180-186.
26. Chen, T., et al., *Conventional MRI features for predicting the clinical outcome of patients with invasive placenta*. Diagn Interv Radiol, 2017. **23**(3): p. 173-179.
27. Ueno, Y., et al., *Evaluation of interobserver variability and diagnostic performance of developed MRI-based radiological scoring system for invasive placenta previa*. J Magn Reson Imaging, 2016. **44**(3): p. 573-83.
28. Bailit, J.L., et al., *Morbidly adherent placenta treatments and outcomes*. Obstet Gynecol, 2015. **125**(3): p. 683-9.
29. Committee on Practice, B.-O., *Practice Bulletin No. 183: Postpartum Hemorrhage.* Obstet Gynecol, 2017. **130**(4): p. e168-e186.
30. Noda, Y., et al., *Prenatal MR imaging diagnosis of placental invasion*. Abdom Imaging, 2015. **40**(5): p. 1273-8.